$Id : ms.tex, v1.112001/09/0421 : 08 : 23 kaiceExp$

USA Observation of Spectral and Timing Evolution During the 2000 Outburst of XTE J1550−564

K. T. Reilly[1], E. D. Bloom, W. Focke, B. Giebels, G. Godfrey, P. M. Saz Parkinson, G. Shabad

Stanford Linear Accelerator Center, Stanford University, Stanford, CA 94309

P. S. Ray[2], R. M. Bandyopadhyay[3], K. S. Wood, M. T. Wolff, G. G. Fritz[4], P. Hertz[5], M. P. Kowalski, M. N. Lovellette, D. J. Yentis

E. O. Hulburt Center for Space Research, Naval Research Laboratory, Washington, DC 20375

and

Jeffrey D. Scargle

Space Science Division, NASA/Ames Research Center, Moffett Field, CA 94305-1000

ABSTRACT

We report on timing and spectral observations of the 2000 outburst of XTE J1550−564 made by the Unconventional Stellar Aspect (USA) Experiment on board the *Advanced Research and Global Observation Satellite* (ARGOS). We observe a low-frequency quasi-periodic oscillation (LFQPO) with a centroid frequency that tends to increase with increasing flux and a fractional rms amplitude which is correlated with the hardness ratio. Several high-frequency quasi-periodic oscillations (HFQPO) were detected by RXTE, during periods where the LFQPO is seen to be weakening or not detectable at all. The evolution of the hardness

[1]Kaice.Reilly@slac.stanford.edu

[2]Paul.Ray@nrl.navy.mil

[3]NRL/NRC Research Associate

[4]Current Address: Praxis Inc., 2200 Mill Rd, 5th Floor, Alexandria, VA 22314

[5]Current address: Office of Space Science, NASA Headquarters, Washington, DC 20546

ratio (4–16 keV/1–4 keV) with time and source flux is examined. The hardness-intensity diagram (HID) shows a cyclical movement in the clockwise direction and possibly indicates the presence of two independent accretion flows: a thin disk and a hot sub-Keplerian flow.

1. Introduction

XTE J1550−564 was first observed in 1998 September by the All Sky Monitor (ASM) on board the *Rossi X-ray Timing Explorer* (RXTE) when it began an outburst lasting approximately 8 months (Smith 1998). XTE J1550−564 began a second outburst on 2000 April 2 (Masetti & Soria 2000), lasting approximately 2 months. The source was detected for a third time in 2001 January but did not go into a full outburst (Tomsick et al. 2001b; Jain et al. 2001b).

Recent optical observations of XTE J1550−564 have placed a lower limit of $7.4 \pm 0.7 M_{\odot}$ on the mass of the compact object (Orosz et al. 2001). This mass places the compact object well above the maximum mass for a stable neutron star and so provides compelling evidence that XTE J1550−564 contains a black hole. During its 1998–1999 outburst, apparent superluminal radio jets ($v > 2c$) were observed by Hannikainen et al. (2001); however, the jet's angle to the line of sight has not yet been determined. Radio and optical observations of the 2000 outburst also show evidence of jet formation (Corbel et al. 2001; Jain et al. 2001).

Complex timing and spectral behavior has been observed by RXTE in XTE J1550−564 during its two full outbursts. This behavior includes detections of three classes of low-frequency quasi-periodic oscillations (< 20 Hz) (LFQPO) and several detections of high frequency QPOs (> 100 Hz) (HFQPO) (Remillard et al. 2001; Miller et al. 2001; Kalemci et al. 2001). Further, color-color diagrams and hardness intensity diagrams of the 1998–1999 outburst showed separate spectral branches for each of the black hole states as well as correlations with quasi-periodic oscillations and other timing behavior (Homan et al. 2001).

During the 1998–1999 outburst, XTE J1550−564 exhibited all four identified black hole spectral states (Sobczak et al. 2000; Homan et al. 2001). In the 2000 outburst the source never achieved the high state (HS), going from an initial low/hard state (LS) to an intermediate state (IS) or a very high state (VHS) and returning to a final LS (Miller et al. 2001). Although previous authors have made a distinction between the IS and VHS, recent work on XTE J1550−564 has suggested that the IS and VHS are actually the same state at different X-ray flux levels (Homan et al. 2001). Therefore, for the remainder of this paper we will refer to this state as the IS. The transition from the initial LS to the IS was made on 2000 April

26 (MJD 51660). The midpoint of transition from the IS to the final LS occurred on May 18 (MJD 51682) (Tomsick et al. 2001a). The observations of Tomsick et al. (2001a) show a clear drop in the soft component and a hardening of the power law component, indicating a transition to the final LS, which was then followed by spectral evolution during the final LS.

In this *Letter*, we report on X-ray observations of the 2000 outburst of XTE J1550−564 made by the Unconventional Stellar Aspect (USA) Experiment on the US Air Force *Advanced Research and Global Observation Satellite* (ARGOS). For a detailed description of the USA experiment see Ray et al. (1999), Wood et al. (2000), and Shabad (2000). We present lightcurves and hardness ratios and track a low frequency QPO which appears in the initial and late stages of the outburst.

2. Observations and Data Analysis

2.1. Lightcurves and Hardness Ratios

The USA Experiment observed XTE J1550−564 at the rate of 2–8 times per day between 2000 April 14 (MJD 51648) and June 18 (MJD 51713). For the present investigation, 193 observations were used, from which we selected ~ 49 ks of data obtained in low-background regions. The data are time tagged, having 32 μs time resolution, and cover an energy range of approximately 1–17 keV in 16 pulse height analyzer (PHA) channels. In this work we do not make use of the lowest (channel 0) and highest (channel 15) PHA channel. We refer to PHA channels 1–14 ($\sim 1 - 16$ keV) as the total range.

To create the light curves shown in Figure 1, a first order background subtraction was made by averaging blank sky observations and then subtracting these values from the count rate. To determine the total error, the standard deviation of the average in the background was added in quadrature to the error on the count rate. USA data were then corrected for obscuration by the instrument support structure and the collimator response. The overall average light curve (normalized to the USA Crab counting rate) for the total range is shown in panel (a) of Figure 1. The circles are RXTE/ASM daily averaged data used to give the complete outburst profile (USA observations did not cover the first few days of the outburst). The USA data points shown are an average of several USA observations. The number of observations averaged was dependent on the observation spacing and signal to noise ratio.

The spectral characteristics of the outburst were studied by dividing the USA data into two energy bands, USA PHA channels 1–3 and channels 4–14. These two bands correspond to 1–4 keV and 4–16 keV, respectively. For the remainder of this *Letter* these bands will

be referred to as the soft band count rate (SB) and the hard band count rate (HB). The motivation for choosing the specific energy ranges of the SB and HB came from properties of the hardness-intensity diagram (HID). During the outburst, XTE J1550−564 traces a cyclic pattern in the HID. Plots of count rates versus the total range show this cyclical structure for individual channels in the range 4–14, but not for channels 1, 2 or 3.

Panels (b) and (c) of Figure 1 show the SB and HB as a function of time during the outburst. The bottom panel of Figure 1 shows the evolution of hardness ratio using these energy bands. The HID in Figure 2 shows how the hardness ratio evolves with total count rate during the outburst. The hardness ratio is plotted only for USA data prior to MJD 51687, after which the signal to noise decreases to the point that the hardness ratio is not constrained. In Figure 2 and panel (f) of Figure 1, one point is shown for each point in panels (b) and (c) of Figure 1.

The design of the USA detector incorporated automatic gain stabilization hardware and frequent iron source energy calibrations were done while in orbit. We note that the USA channel to energy conversion varies slightly over the USA orbit; however, checks performed showed that this variation made no significant impact on the relevant features seen in the SB, HB, and hardness ratio. A further check of our spectral results was made by comparing our data to public RXTE/ASM data. Daily averaged ASM data were used to find the hardness ratio as a function of time and to make a HID. The ASM hardness ratio was calculated by dividing the sum of ASM B Band (3–5 keV) and C Band (5–12 keV) by A Band (1.5–3 keV). To try to emulate the ASM energy bands the USA PHA channels 3–11 (3–11.5 keV) were summed and divided by channel 2 (2–3 keV). The ASM data confirmed the hardness ratio observed with USA and the cyclic behavior in the HID.

2.2. Power Spectra: Low Frequency QPOs

A low frequency quasi-periodic oscillation (LFQPO) was ubiquitous during the rise of the outburst and during the decay of the outburst after the secondary maximum. In order to track the LFQPO evolution through the outburst, observations were grouped by day and frequently in sub-day groups (signal to noise ratio permitting).

Power spectra (see Nowak et al. 1999 and references therein) were calculated from these groups and averaged. The resultant power spectrum for each group containing a LFQPO was fit with a power law or broken power law and a Lorentzian for any observable QPO features. Fits were made in three energy bands: the total range, SB, and HB. In case of confusion by sub-harmonics, the strongest QPO feature was chosen as the primary LFQPO

(see Remillard et al. 2001). In most cases no sub-harmonics were detectable. Panel (d) of Figure 1 shows how the centroid frequency of the LFQPO evolves during the outburst. The evolution of the rms amplitude for all three energy bands is shown in panel (e). Panels (d) and (e) show error bars calculated by allowing the χ^2 of the fit to vary by one. All error bars are given at the 68% confidence level.

3. Results

3.1. QPO Evolution and Correlation to State Changes

We observe LFQPOs between MJD 51648 and 51663 and between MJD 51675 and 51686 which vary in frequency between 0.24–7.19 Hz and 6.34–0.64 Hz, respectively. During the times of these detections the source is either in the LS or near the transition from one state to another. The LFQPO rms amplitude decreases rapidly at the state transition from the LS to the IS and then increases during the transition back to the LS, indicating that the mechanism for creating the LFQPO is suppressed in the IS. The LFQPO centroid frequency generally increases with increasing flux; the fractional rms amplitude is correlated with hardness ratio (see Figure 1).

During the IS, significant detections of HFQPOs (249–278 Hz) were made by RXTE between between MJD 51663 and 51675 (Miller et al. 2001). A 65 Hz QPO has been discovered by Kalemci et al. (2001) at MJD 51684.8. These HFQPO detections occurred during the periods where USA observed the LFQPO to be weakening or not detectable at all. It is interesting to note that the HFQPOs were observed to decrease in significance as a function of time in the IS (Miller et al. 2001). We observe a decline in rms amplitude of the LFQPO near the LS/IS transition, which marks the approximate onset of the HFQPOs. Towards the end of the IS, near the IS/LS transition, the HFQPO weakens as the LFQPO once again becomes detectable. This trend continues in the last days of the outburst, when the LFQPO rms amplitude weakens and the 65 Hz QPO is detected.

These QPO features are qualitatively consistent with observations of XTE J1550−564 during the 1998–1999 outburst (Remillard et al. 2001), during which an "antagonism" between LFQPOs and HFQPOs was also observed. During that outburst, type "C" QPOs were observed when strong correlations were seen between the frequency and disk flux while the amplitude was observed to correlate with disk temperature (Remillard et al. 2001). These previous observations closely resemble what we see for the LFQPO observed during the 2000 outburst; thus we tentatively classify the LFQPO discussed here as a type C.

At MJD 51661.21 an anomalous QPO was detectable exclusively in the HB, in contrast

to the primary LFQPO which appears in all energy ranges. In Figure 1 panel (d), this anomalous QPO is the highest frequency point and is marked with a large unfilled circle near MJD 51660. This QPO was detected between the primary LFQPO and its harmonic and has a frequency of $7.19^{+0.12}_{-0.11}$ Hz, whereas the primary LFQPO is seen at 4.71 ± 0.05 Hz and its harmonic is seen at $9.75^{+0.4}_{-0.35}$ Hz.

3.2. Spectral Evolution

From Figure 1 it is clear that the 2000 outburst of XTE J1550−564 does not follow the canonical fast rise, exponential decay (FRED) outburst as would have been expected prior to the RXTE era. Now, with many more examples of well-observed soft X-ray transient (SXT) outbursts, it has become clear that few outbursts look like pure FREDs, and that the outburst profile can be very different at high energy than at low energy. Comparing the SB and HB lightcurves in Figure 1 (b) and (c), the two bands rise approximately in unison, but show very different behavior after the peak. With the exclusion of the secondary maximum the HB light curve shows a nearly symmetric outburst profile, while the SB rapidly rises, then decays approximately linearly. As is often observed in SXTs, the decay returns to its original path after the secondary maximum.

In the HID (Figure 2), we observe that the difference between the SB and HB lightcurves manifests itself as a cyclic structure that moves with time in a clockwise direction. The HID shows a rapid drop in the hardness ratio as the source enters the IS and a rapid increase as the final LS is realized. This type of spectral structure, which has been seen in several other sources (Smith et al. 2001), is a consequence of the spectrum being harder during the rise than during the decline.

4. Discussion: Two Flow Models

The different behavior of the HB and SB lightcurves, together with the lack of a strict correlation between the QPO frequency and source flux, suggest a scenario involving a two component accretion flow. Models invoking two *independent* accretion flows (*e.g.* a thin disk and a hot sub-Keplerian flow) have been described by Chakrabarti & Titarchuk (1995) and Smith et al. (2001), while van der Klis (2001) presents a model where the two parameters are the instantaneous and time averaged values of a *single* quantity.

Whether the two accretion parameters are dependent or independent, there will be a transition radius at which the Keplerian disk is disrupted and forms a hot sub-Keplerian

flow. This inner flow can be an advection-dominated accretion flow (Esin et al. 1997) or a postshock flow interior to the radius where two independent flows interact (Chakrabarti & Titarchuk 1995). This transition radius is a natural site to consider for the formation of low or high frequency QPOs. The relationship between the Keplerian orbital period and radius for a $7.5M_{\odot}$ black hole is $R \sim 132 R_{\rm Sch} P^{2/3}$, where $R_{\rm Sch}$ is the Schwartzchild radius ($R_{\rm Sch} \sim 22.1$ km for a $7.5M_{\odot}$ black hole) and P is the orbital period in seconds. For small values of the transition radius, one can consider models where the high-frequency QPO is the Keplerian orbital period at the transition radius and the LFQPO is related to radial oscillations of the transition layer as described by Titarchuk & Osherovich (1999). For large values of the transition radius, the LFQPO could be the Keplerian frequency, but then another explanation is required for the HFQPO which, at least in some instances, are seen simultaneously.

In order for a two flow model to explain the spectral characteristics described in § 3.2, it should allow for spectral softening to occur while the overall source flux is dropping. For two independent flows, this type of spectral evolution occurs because changes in the radial flow may occur on a short (free-fall) timescale, while the effect of changes in the the disk accretion rate are delayed due to viscosity (Chakrabarti & Titarchuk 1995; Smith et al. 2001). A model of two independent flows was applied to GRS 1758−258 and 1E 1740.7−2942 by Smith et al. (2001), both of which also showed spectral softening with decreasing flux. Using a dependent flow model, van der Klis (2001) suggests that if the count rate is dominated by the disk accretion rate and the spectral hardness is related to the inner disk radius (which is determined by the time-averaged accretion rate), the same cyclic structure in the HID will result.

Recent ideas on the role of jets in microquasars suggest a link between the jet and the corona (see Fender 2001 and references therein). The LS is associated with a continuous radio-emitting outflow and the presence of the strong LFQPO. At the transition to the IS, discrete radio ejections seem to be common but the continuous jet ceases and the LFQPO mechanism is suppressed. This indicates that both the outflow and the LFQPO are characteristic of the LS and are related to the presence of a hot corona. The accretion-ejection instability model provides a mechanism where spiral density waves may be responsible for both the LFQPO and energizing the jet(Tagger & Pellat 1999).

Continued theoretical development and application to the body of observations of XTE J1550−564 may allow a final determination of the true LFQPO mechanism, the cause of the spectral state changes, and the means of jet production.

We gratefully acknowledge useful discussions with Lev Titarchuk. We thank Mark

Yashar for providing useful references and Emrah Kalemci for useful comments on our discussion. Work at SLAC was supported by department of Energy contract DE-AC03-76SF00515. Basic research in X-ray Astronomy at the Naval Research Laboratory is supported by ONR/NRL. This work was performed while RMB held a National Research Council Research Associateship Award at NRL. JDS is grateful to the NASA Applied Information Technology Research Program for support. This paper made use of quick-look results provided by the ASM/RXTE team (see http://xte.mit.edu).

REFERENCES

Chakrabarti, S. & Titarchuk, L. G. 1995, ApJ, 455, 623

Corbel, S., Kaaret, P., Jain, R. K. et al. 2001, ApJ, 554, 43

Esin, A. A., McClintock, J. E., & Narayan, R. 1997, ApJ, 489, 865

Fender, R. 2001, Proc. International Symposium on High Energy Gamma-Ray Astronomy, Heidelberg, Eds. F. Aharonian & H. Voelk, 2001, AIP, in press, 1233

Hannikainen, D. et al. 2001, Proc. of the 4th INTEGRAL Workshop, Alicante, 2070

Homan, J., Wijnands, R., van der Klis, M., Belloni, T., van Paradijs, J., Klein-Wolt, M., Fender, R., & Méndez, M. 2001, ApJS, 132, 377

Jain, R. K., Bailyn, C. D., Orosz, J. A., McClintock, J. E., & Remillard, R. A. 2001, ApJ, 554, L181

Jain, R., Bailyn, C., & Tomsick, J. 2001, IAU Circ., 7575, 3

Kalemci, E., Tomsick, J. A., Rothschild, R. E., Pottschmidt, K., & Kaaret, P. 2001, ApJ, submitted (astro-ph/0105395)

Masetti, N. & Soria, R. 2000, IAU Circ., 7399

Miller, J. M. et al. 2001, ApJ, submitted (astro-ph/0105371)

Nowak, M. A., Vaughan, B. A., Wilms, J., Dove, J. B., & Begelman, M. C. 1999, ApJ, 510, 874

Orosz, J. A., van der Klis, M., McClintock, J., Bailyn, C., & Remillard, R. 2001, The Astronomer's Telegram, 70

Ray, P. S. et al. 1999, in X-ray Astronomy 1999, Bologna, Italy, in press (astro-ph/9911236)

Remillard, R. A., Sobczak, G. J., Muno, M. P., & McClintock, J. E. 2001, ApJ, submitted, (astro-ph/0105508)

Shabad, G. 2000, Stanford Ph.D. Thesis, SLAC Report No. 562

Smith, D. A. 1998, IAU Circ., 7008

Smith, D. M., Heindl, W. A., & Swank, J. H. 2001, ApJ, submitted (astro-ph/0103304)

Sobczak, G. J., McClintock, J. E., Remillard, R. A., Cui, W., Levine, A. M., Morgan, E. H., Orosz, J. A., & Bailyn, C. D. 2000, ApJ, 544, 993

Tagger, M. & Pellat, R. 1999, A&A, 349, 1003

Titarchuk, L. & Osherovich, V. 1999, ApJ, 518, L95

Tomsick, J. A., Corbel, S., & Kaaret, P. 2001, ApJaccepted (astro-ph/0105394)

Tomsick, J. A., Smith, E., Swank, J., Wijnands, R., & Homan, J. 2001, IAU Circ., 7575, 2

van der Klis, M. 2001, ApJ, in press (astro-ph/0106291)

Wood, K., Ray, P. S., Bandyopadhyay, R. M., et al. 2000, ApJ, 544, L45

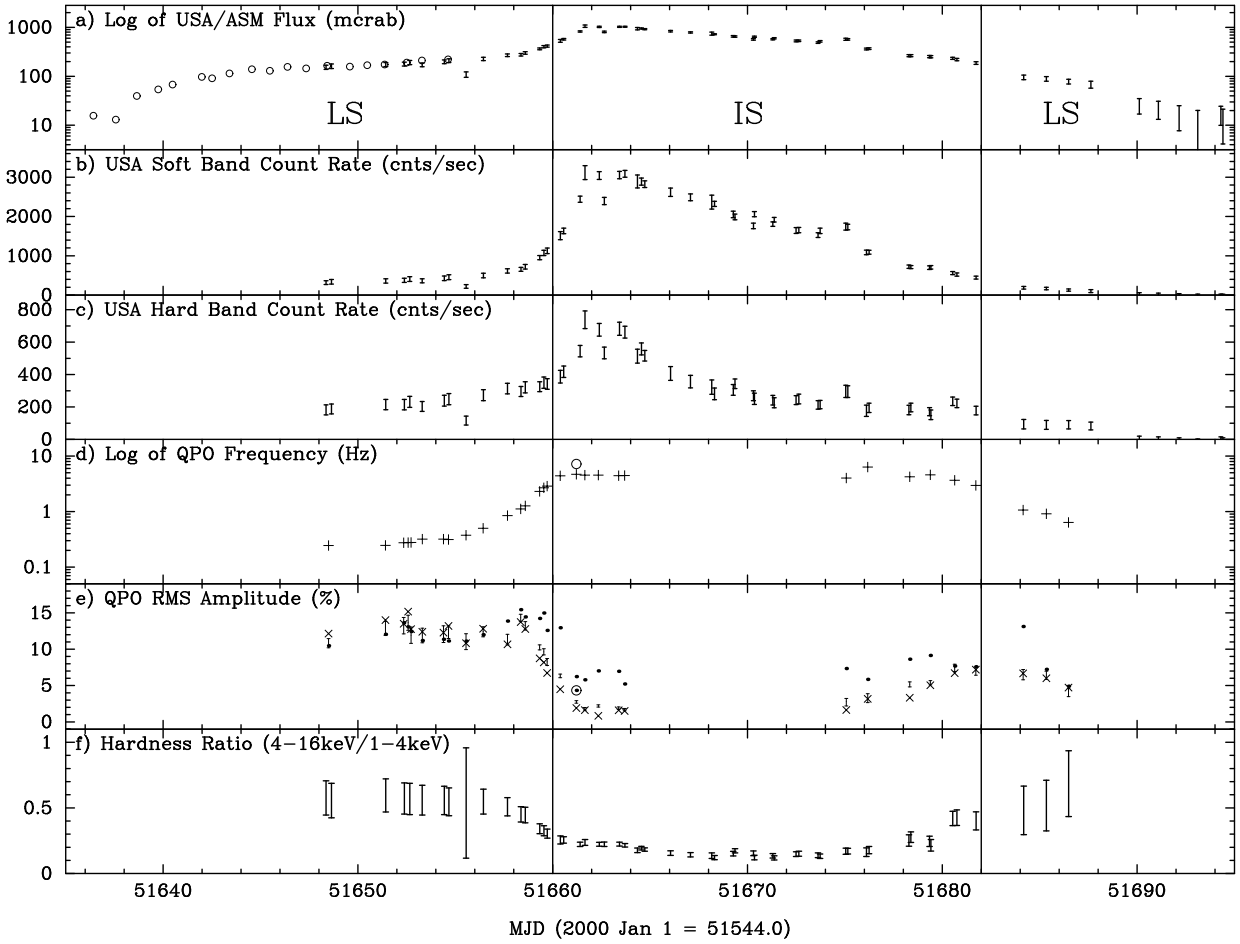

Fig. 1.— Time Evolution of XTE J1550−564. The solid vertical lines show the time of transition between states. Panels: (a) USA/ASM Crab normalized fluxes for the outburst on a log scale. The circles are ASM daily averaged data taken before USA started observations. ASM error bars, not shown, are smaller than the circles. USA data are shown as error bars only. (b) USA Soft Band count rate (SB), $\sim 1-4$ keV. (c) USA Hard Band count rate (HB), $\sim 4-16$ keV. (d) LFQPO centroid frequency on a log scale. The plus signs show results for the total range 1–16 keV. The large unfilled circle shows the frequency of the anomalous HB QPO. Error bars, not shown, are smaller than the symbol size. (e) LFQPO percent rms amplitude. The total range 1–16 keV is represented by error bars only. Filled circles are the HB and the "X"s are the SB. The large unfilled circle marks the anomalous QPO. Error bars in the SB and HB are not shown, but are comparable to those on the total range. (f) Hardness ratio (HB/SB).

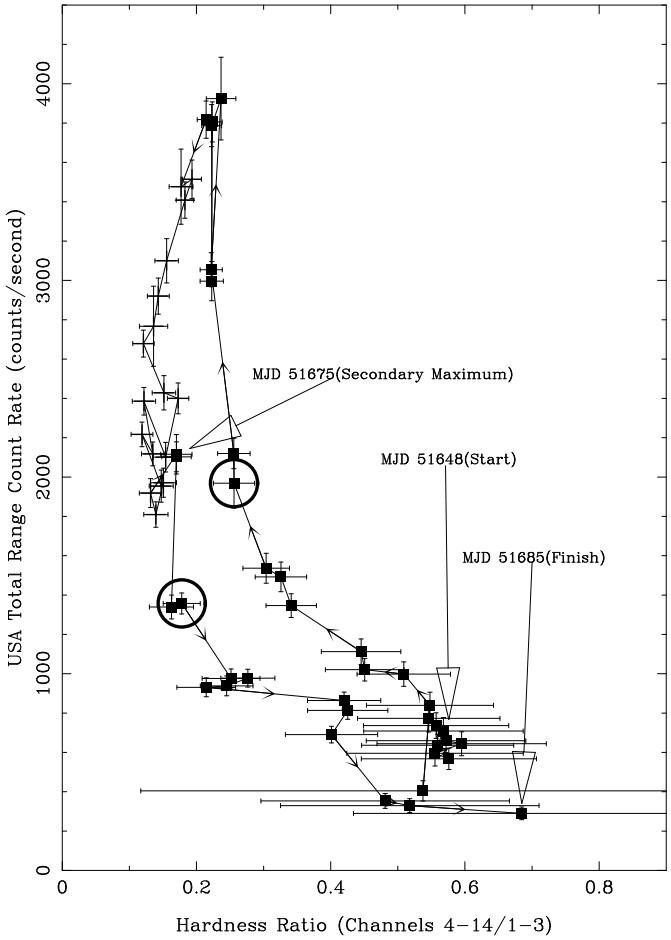

Fig. 2.— Total Range Count Rate vs. Hardness Ratio (HB/SB). Squares are plotted on points in which the LFQPO was detected. Points at which no QPO detection was made only show error bars. The error bars shown are the standard deviation of the flux and the hardness ratio. Arrows plotted between points show the direction of time. The larger outlined arrows mark the start and stop times of USA observations and the time of the secondary maximum. Transitions between states have been marked with the bold circles.